

Altered magnetism and new electronic length scales in magneto-electric
 $\text{La}_{2/3}\text{Sr}_{1/3}\text{MnO}_3\text{-BiFeO}_3$ heterointerface

This content has been downloaded from IOPscience. Please scroll down to see the full text.

2013 New J. Phys. 15 113042

(<http://iopscience.iop.org/1367-2630/15/11/113042>)

View [the table of contents for this issue](#), or go to the [journal homepage](#) for more

Download details:

IP Address: 131.230.106.30

This content was downloaded on 21/01/2015 at 20:16

Please note that [terms and conditions apply](#).

Altered magnetism and new electronic length scales in magneto-electric $\text{La}_{2/3}\text{Sr}_{1/3}\text{MnO}_3$ – BiFeO_3 heterointerface

S K Mishra¹, D Mazumdar², K Tarafdar³, Lin-Wang Wang³,
S D Kevan^{1,4}, C Sanchez-Hanke⁵, A Gupta² and S Roy^{1,6}

¹ Advanced Light Source, Lawrence Berkeley National Laboratory, Berkeley, CA 94720, USA

² Center for Materials for Information Technology, The University of Alabama, Tuscaloosa, AL 35487, USA

³ Materials Science Division, Lawrence Berkeley National Laboratory, Berkeley, CA 94720, USA

⁴ Department of Physics, University of Oregon, Eugene, OR 97401, USA

⁵ National Synchrotron Light Source, Brookhaven National Laboratory, Upton, NY 11973, USA

E-mail: SRoy@lbl.gov

New Journal of Physics **15** (2013) 113042 (11pp)

Received 22 May 2013

Published 20 November 2013

Online at <http://www.njp.org/>


doi:10.1088/1367-2630/15/11/113042

Abstract. We map out the charge-spin density profile of magneto-electric $\text{La}_{2/3}\text{Sr}_{1/3}\text{MnO}_3$ (LSMO)– BiFeO_3 (BFO) heterostructure using soft x-ray resonant magnetic reflectivity. We show that the spatial extent of interface orbitals can extend over a few lattice periods even for an atomically sharp interface. While LSMO magnetization is depleted at the interface, BFO does develop a weak magnetic moment mostly near the interface, probably due to a proximity-induced charge-transfer process. Our study reveals that simultaneous control of electronic and magnetic interfaces is essential in realizing the potential of oxide devices.

⁶ Author to whom any correspondence should be addressed.



Content from this work may be used under the terms of the [Creative Commons Attribution 3.0 licence](https://creativecommons.org/licenses/by/3.0/). Any further distribution of this work must maintain attribution to the author(s) and the title of the work, journal citation and DOI.

 Online supplementary data available from stacks.iop.org/NJP/15/113042/mmedia

Contents

1. Introduction	2
2. Experimental procedures	3
3. Discussions	3
3.1. Hard x-ray reflectivity	3
3.2. Soft x-ray reflectivity	5
4. Theoretical calculations	8
5. Conclusion	9
Acknowledgments	10
References	10

1. Introduction

Quantitative investigation of orbital and magnetic distribution at complex-oxide interfaces is pivotal for proper understanding of the competing interactions that lead to novel functionalities. A multitude of discoveries have been reported at complex-oxide interfaces, which has shifted the paradigm of engineering functionalities away from the bulk. Discovery of tunable two-dimensional electron gas [1, 2], magnetism [3] and superconductivity [4] at the LaAlO_3 – SrTiO_3 (STO) interface, enhancement of ordering temperature in a magnetic superlattice [5], orbital reconstruction at a superconductor–ferromagnet interface [6, 7] and creation of a magneto-electric heterostructure [8], for example, necessitates interface-specific investigations. The key lies in understanding and achieving control over various factors such as symmetry breaking, frustration, charge transfer, electrostatic coupling, epitaxial strain etc that influence the interfacial ground state. Therefore, determining the magneto-chemical depth profile in such heterostructures will provide vital insight into the spin and electronic structure essential for realizing devices based on oxide interface properties [9, 10].

We investigate here the magnetic and electronic density profile of a model magneto-electric heterostructure comprising of ferromagnetic $\text{La}_{2/3}\text{Sr}_{1/3}\text{MnO}_3$ (LSMO) and antiferromagnetic–ferroelectric BiFeO_3 (BFO) grown on (001) oriented STO. Both LSMO ($T_c = 370$ K) and BFO ($T_N = 370$ K, ferroelectric $T_c = 820$ K) attract wide interest as they retain their primary functionality at room temperature. One of the desired outcomes is a strong magneto-electric coupling between the ferromagnetic and ferroelectric order parameters which can be enhanced at the interface. Recent exciting reports of electric field control of magnetism [19–21] and exchange bias [22] in ferromagnetic–ferroelectric heterostructures further motivations our investigation. Apart from these rich phenomenologies exhibited by LSMO–BFO heterostructure, it has also been proposed as an interesting system for magnetic tunnel junctions [17]. This depth-dependent study also allows us to investigate another important oxide interface, between LSMO and the STO substrate. Even though this interface is reported to have high spin-polarization [11–13], its magnetic interface has surprisingly remained controversial [14–16]. The orbital interface is an even bigger, open question.

In this paper, we report on new manifestations of complex functionalities emerging at the magneto-electric heterointerface. We show that the electronic and/or orbital reconstruction occurring at oxide interfaces have more length scales than previously anticipated and we demonstrate this in LSMO–BFO heterostructure. The magnetic profile is equally intriguing and experimental findings provide new insights into some of the long speculated issues of interface magnetism of LSMO. Direct observation of the depleted interface magnetism of LSMO (as has been speculated only as a ‘dead layer’) has been demonstrated at the interface that can span over 2–3 nm. Our measurements also reveal that the first few interfacial layers of antiferromagnetic BFO can develop a very weak ferromagnetic moment in proximity with LSMO. The experimental results are discussed in the framework of heterogeneous magneto-electric interface and orbital selective charge transfer effects. These experimental and theoretical findings provide unprecedented detail of the complex phenomena occurring at buried magneto-electric heterointerfaces that is essential for assessing the potential functionalities of these systems for the next generation nano-electronics applications.

2. Experimental procedures

An epitaxial LSMO–BFO heterostructure was grown on (001)-oriented atomically flat SrTiO₃ substrates using the pulsed laser deposition method with a KrF excimer laser ($\lambda = 248$ nm) at a fluence of 1.5–2.0 J cm⁻². Both layers were grown at 700 C substrate temperature. Background oxygen pressure for LSMO was 200 mtorr with a 2 Hz laser pulse repetition rate while for BFO the oxygen pressure was 100 mtorr and 10 Hz repetition rate. The growth rate was controlled through *ex situ* x-ray reflectivity calibration and was 40–50 pulses nm⁻¹ for both LSMO and BFO. Detailed BFO growth and characterization can be found elsewhere [18]. Resonant x-ray magnetic reflectometry measurements were carried out at the fast polarization switching beamline, X13A, of National Synchrotron Light Source (NSLS), Brookhaven National Laboratory, USA and Beamline 12.0.2.2 of the Advanced Light Source (ALS), Lawrence Berkeley National Laboratory, USA. Resonant x-ray profiles at a fixed angle were measured using both circular and linear polarized incident x-ray beams. Incoming right (I⁺) and left (I⁻) circularly polarized x-ray beams were tuned to the Mn L₃ (639.5 eV) and Fe L₃ (707.0 eV), respectively. At first, specular reflectivity was measured at a fixed incidence angle of 16° as a function of incident beam energy at an applied field of 350 Oe. Element specific hysteresis loops were measured at 300 K (room temperature) and 32 K. In a second set of experiments specular magnetic reflectivity was measured at 300 and 32 K at both the Mn and Fe edges and the asymmetry ratio ($A_{\text{asym}} = (I^+ - I^-)/(I^+ + I^-)$) determined. The measurements were done as a function of wave vector transfer q_z with 350 Oe magnetic field applied along the x-ray propagation direction.

3. Discussions

3.1. Hard x-ray reflectivity

The structural interface of the LSMO–BFO heterostructure was characterized by x-ray reflectivity measurements with Cu K α ($\lambda = 0.154$ 18 nm) radiation as shown in figure 1(a). The reflectivity curve was fitted based on the Parratt [27] formalism incorporating the effect of the roughness according to Nevot and Croce [28] to obtain values for thickness and structural

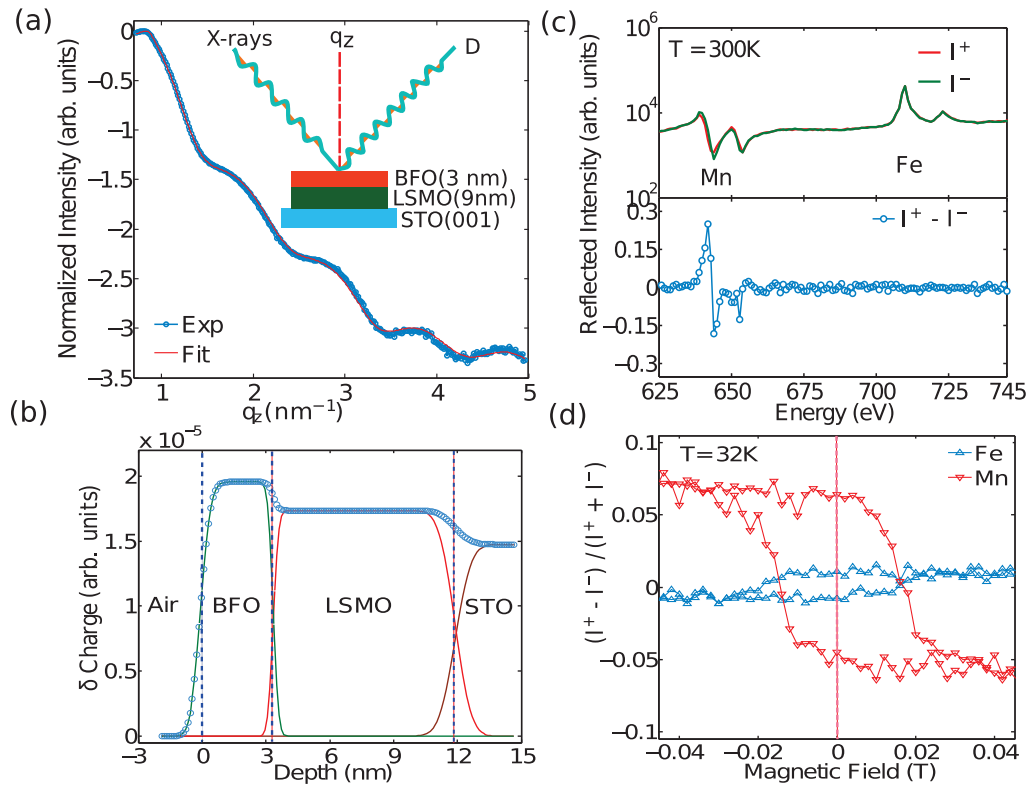


Figure 1. (a) Cu K_{α} x-ray reflectivity data (circles) and fits (solid line). The inset shows the geometry of the soft x-ray experimental set up, where a beam of circularly polarized x-ray is incident on the sample. A magnetic field of 350 Oe is applied along the beam direction. The detector angle is at twice the incident angle to satisfy the specular reflectivity condition. (b) Charge density profile of the heterostructure obtained from the fits of the reflectivity curve as shown in figure (a). The dotted blue lines represent the structural interface of oxide heterostructures. (c) Reflected intensity as a function of incident photon energy for the circularly left (I^+) and right (I^-) helicities of incident light (upper panel). At 300 K magnetic dichroic signal is observed only at the Mn L resonance edges. In the limit of experimental resolution no magnetism is observed at the Fe L resonance edges, confirming a robust antiferromagnetic state of BFO at 300 K (lower panel). (d) At 32 K, a very weak but clear hysteresis loop is observed at the Fe L_3 edge indicating the presence of a net spontaneous magnetic moment in BFO, which is exchange coupled to adjacent Mn spins of LSMO.

interfacial roughness of individual layers as illustrated in figure 1(b). The thickness of LSMO (BFO) layer was extracted to be 8.20 (3.40) nm, which nominally corresponds to approximately 21 and 8 unit cells, respectively, in agreement with the pre-calibrated values. The structural roughness at the LSMO–BFO (LSMO–STO) interface was determined to be 0.20 ± 0.01 (0.59 ± 0.02) nm indicative of atomically sharp interfaces. We note here that the roughness is the root mean square value averaged in the interface plane over macroscopic areas of the sample covered by the footprint of the x-ray beam.

3.2. Soft x-ray reflectivity

Resonant soft x-ray magnetic reflectivity measurements using a circularly polarized incident x-ray beam (I^+ , I^-) is a powerful non-invasive probe, where we directly measure the Fourier components of the chemical specific charge and magnetization density distribution. By measuring a large set of Fourier components as a function of wave vector transfer q_z ($= 2 * \pi/d$, where d is the real space length scale), we can accurately determine depth-dependent charge and magnetization density profiles in real space and uniquely identify the interfacial electronic and spin structure [23–25]. The resonant nature of the technique provides unprecedented sensitivity in detecting small changes in refractive index. The sum signal ($I^+ + I^-$) is dominant by charge or electronic signatures, while the asymmetry ratio ($(I^+ - I^-)/(I^+ + I^-)$) represents interference of charge and magnetic scattering factors, and is linearly proportional to magnetization. By analyzing the sum signal we can therefore extract quantitative electronic densities while the magnetization profile is obtained by analyzing the difference signal [26].

In order to determine resonant energies we measured the reflected intensity as a function of incident x-ray energy with the detector setting of 16° that show peaks related to Mn and Fe L_3 edges (figure 1(c)). Presence (absence) of a Mn (Fe) magnetic dichroic signal indicates that LSMO is magnetic but BFO has no net moment at 300 K. Element specific hysteresis loop measurements at the Mn (Fe) L_3 edge 639.5 eV (707.0 eV) also show similar results. At 32 K both magnetization and coercivity of LSMO are significantly enhanced compared to 300 K measurements, as expected. Interestingly enough, we also find a spontaneous magnetization at the Fe edge indicating a very weak ferromagnetic behavior of BFO (figure 1(d)). Further, the similarity of coercive fields for Fe and Mn loops indicates likely exchange coupling between Fe and Mn spins. We note here that in reflection geometry, only one hysteresis curve at a fixed q_z is not sufficient to determine the sign of exchange coupling. As we show below, such information can only be extracted after a rigorous analysis of the magnetic reflectivity curves.

Figures 2(a) and (b) illustrate the soft x-ray resonant reflectivity sum signal ($I^+ + I^-$) as a function of the wave vector transfer q_z at both the Mn and Fe L_3 edges. Resonant sensitivity is clear from inspection as the lineshapes are quite different. To analyze and extract relevant information we fit the data using rigorous scattering theory employing distorted wave born approximation [26]. Due to the high sensitivity of resonant soft x-rays to small chemical-specific changes in electron densities particularly near the interfaces, we found that a simple three layer model was not sufficient to fit the data. In order to reproduce the complex variation of the density profile we mathematically modeled near-interface regions with layers that have slightly different optical constants along with its own roughness which would represent variations in electronic structure. Alternatively, we could have sliced each layer into multiple layers to represent the continuous density variation with its own thickness and roughness. However, that would introduce far more free parameters into fitting. To fit the Fe and Mn reflectivity data satisfactorily required that the near-surface of 0.60 nm region has different optical constants than bulk BFO coupled with transitory layers at the LSMO–BFO (1.50 ± 0.16 nm) and LSMO–STO (1.30 ± 0.22 nm) interface. The roughness at the LSMO–BFO transitory layer was found to be 1.20 ± 0.07 nm, whereas the roughness value at the LSMO–STO transitory layer was 0.50 ± 0.11 nm. We found that the fitting is generally more sensitive to LSMO–BFO interlayer properties than the LSMO–STO interlayer.

The existence of extremely rough interfaces is in stark contrast with our structural characterization and this implies that soft x-rays do not ‘see’ the interfaces to be as sharp

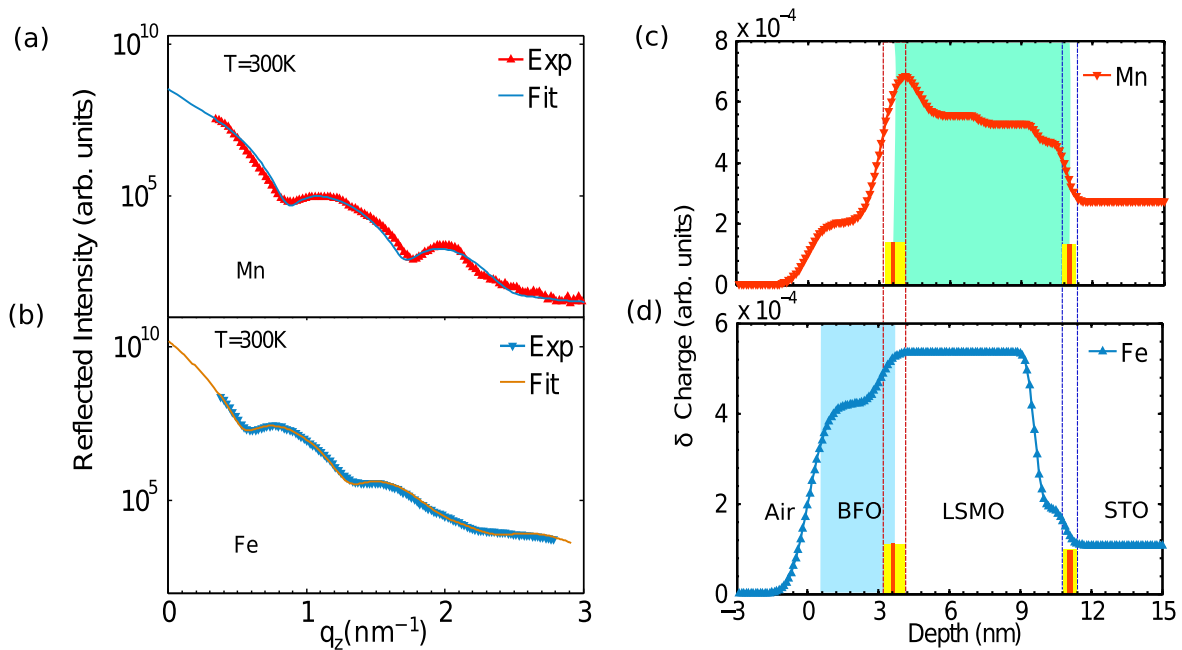


Figure 2. (a), (b) ($I^+ + I^-$) signals (solid lines with triangles) at the Mn(Fe) L_3 resonance edges, which predominantly contains the electronic signature. Fits to the data are shown by solid lines. (c), (d) Variation of the charge density profile along the depth of the interface. Distinctly different electron densities near the interface regions were observed. Fits to the experimental data also suggest that electronic roughness (yellow stripes in figures (c) and (d)) of such transitory layers are different compared to the structural roughness (red stripes).

and abrupt as hard x-rays do. Together, the existence of transitory layers with a high degree of roughness compels us to view these interfaces as electronically heterogeneous i.e. spread over much larger length scales than non-resonant techniques can reveal. Multiple reasons can contribute to the existence of the broad electronic interface. Subtle chemical changes such as variation of the mean oxidation number of Mn and Fe from bulk to interface can directly alter the refractive index at resonances and, therefore, the scattering cross-section. Secondly, structural or orbital reconstruction at the interface due to factors such as symmetry breaking, interfacial Jahn–Teller distortion among others, can also lead to minute changes in refractive index which the soft x-rays at resonances can see due to its electronic sensitivity. It has to be noted that the observed broad electronic interface of over 2–3 atomic lattices implies participation of both Mn and Fe orbitals. This observation is supported in recent findings of suppressed octahedral tilts in LSMO–BFO interfaces [30] which will be picked up in our measurements. At the LSMO–STO layer, considering the propensity of STO to become Sr-deficient and Ti–O rich at the surface, the LSMO–STO transitory layer could be Ti rich [29]. Our finding clearly demonstrates that soft x-rays can provide interfacial electronic information which hard x-rays cannot.

The magnetic depth profile can be probed using asymmetry ratio analysis and is shown in figures 3(d) and (e). Both room and low temperature (32 K) Mn edge magnetic reflectivity show a varying asymmetry ratio as a function of wave vector transfer q_z with 32 K data showing a

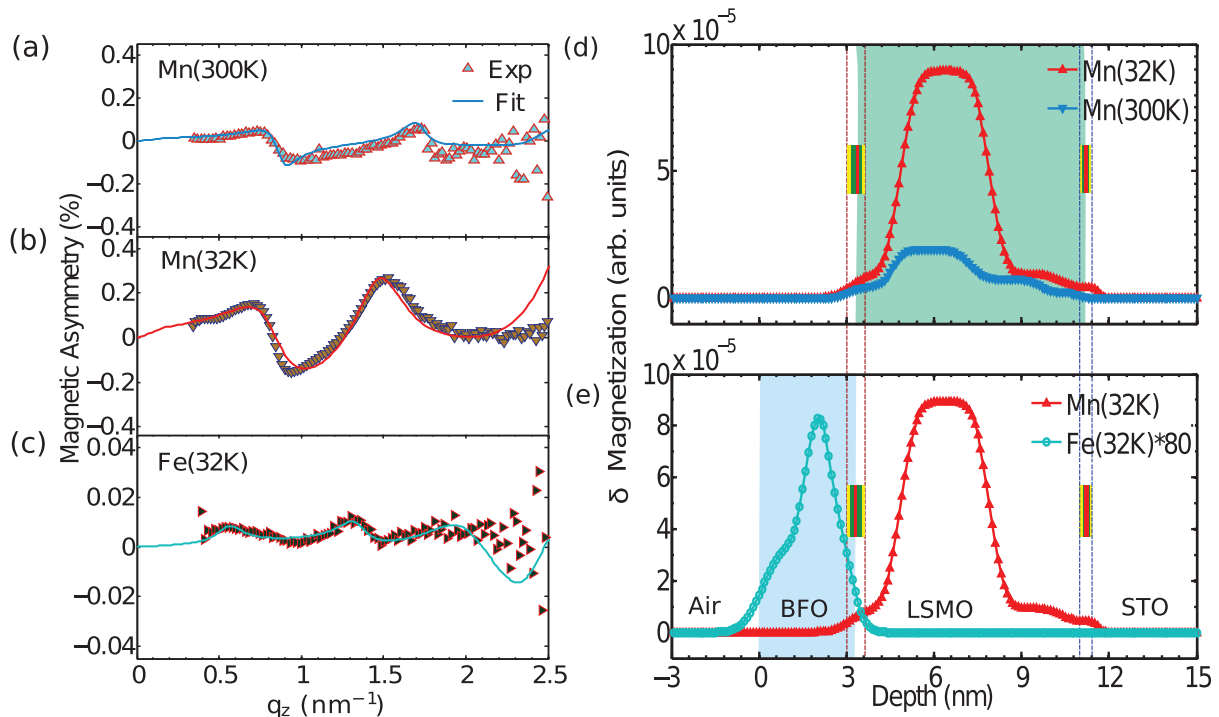


Figure 3. (a), (b) Asymmetry ratio ($(I^+ - I^-)/(I^+ + I^-)$) (solid points) and corresponding fit (solid lines) for the Mn L_3 edge at 300 and 32 K. No asymmetry ratio is observed at 300 K for Fe. An increase in the asymmetry ratio is observed at low temperatures indicating increased magnetization at low temperatures. (c) The asymmetry ratio at the Fe L_3 edge at 32 K. (d) Comparison of Mn magnetic profile at 300 and 32 K, indicating that the Mn magnetization increases mostly in the bulk layers of the film. Significant modifications of the magnetic density profile are observed near the interfaces. (e) Relative comparison of magnetic density profiles of Mn and Fe at 32 K, indicating that Fe magnetization is much weaker compared to Mn and peaks near the LSMO–BFO interface (note Fe magnetic density profile is scaled). Magnetic roughnesses (green stripes) is slightly larger at the LSMO–BFO interface compared to LSMO–STO interface.

75% increase in the asymmetry ratio, consistent with magnetometry data (figures 3(a), (b) and supplementary section S1 (available from stacks.iop.org/NJP/15/113042/mmedia)). In the limit of experimental resolution no magnetic contrast was found for Fe at 300 K. The solid lines in figures 3(a), (b) show that a reasonably good fit to the asymmetry ratios has been achieved. The resulting magnetization profiles reveal that Mn magnetism is weaker at the interfaces and attains the maximum value at the middle of the layer. Furthermore, the suppression of interface magnetism is found to be asymmetric; Mn magnetism falls off well before the nominal LSMO–STO structural interface compared to LSMO–BFO, both at room and low temperature. This is clearly shown in figures 3(d), (e) where we find that the Mn magnetism decreases as the LSMO–BFO structural interface is approached (about 23% less than maximum value at 32 K). The depleted magnetism at LSMO–STO interface extends 1.5 nm into the bulk before slowing recovering to the maximum value at roughly the middle of the LSMO layer. Reduced

magnetism in proximity of the transitory layer appears to be consistent with the supposed ‘dead layer’ formation at oxide interfaces [15]. We also found that the magnetic roughness, which is a metric of spin disorder, is roughly of similar order to charge roughness (0.70 ± 0.1 versus 1.20 ± 0.07 nm at the LSMO–BFO interface) indicative of an intricate link between magnetic and electronic heterogeneities at the interface.

One of the more interesting findings of our study was identifying at low temperatures a small asymmetry ratio ($\sim 0.015\%$) at the Fe-edge which indicates the presence of a net but very weak magnetic moment in the BFO layer (figure 3(c)). The magnetization in the BFO layer peaks within 0.70 nm of the structural BFO–LSMO interface and falls off gradually away from the interface (figure 3(e)). We therefore find that the majority of the net moment in BFO is confined very close to the LSMO–BFO structural interface and is oriented parallel to Mn magnetization in LSMO. The density profile curve of Fe is aligned in the same direction as the Mn curve, which is indicative of parallel alignment of Mn and Fe moments. From the magnetic density profile curve shown in figure 3(e) we can infer that the maximum value of Fe magnetism is $\sim 1.0\%$ of the peak Mn magnetism and $\sim 0.06\%$ of the total magnetization thereby indicating the weakness of the BFO magnetization.

4. Theoretical calculations

To shed light on the origin of interface magnetism of the BFO layer, we performed first-principles density functional theory calculations with on-site Coulomb U correction on a (001)-oriented LSMO–BFO heterostructure. To simultaneously investigate both bulk and interface properties, a large 208 atom supercell was constructed consisting of 6 LSMO unit cell layers and 4 BFO unit cells (see supplementary section figure S2 (available from stacks.iop.org/NJP/15/113042/mmedia) for the near-interface relaxed supercell structure) both constrained in-plane to the lattice parameter value of cubic STO. The interfacial layer consists of four Fe atoms from BFO connected to Mn atoms through oxygen atoms. Two of these four Fe atoms are ferromagnetically (FM) aligned and the other two Fe atoms are antiferromagnetically (AF) aligned with interfacial Mn. Our relaxed structure reveals substantially different structural and electronic properties between bulk and interface BFO. Firstly, we observe an expansion in the out-of-plane lattice parameter for the near interface BFO layers (4.02 \AA) compared to the bulk value (3.96 \AA , data not shown). This is consistent with application of an in-plane compressive strain to the BFO layer through the STO substrate. A slight lattice contraction of the interfacial AF Fe octahedra by about 0.01 \AA compared to the FM Fe octahedra is also observed (see supplementary section S2). The spin-resolved density of states (DOS) of the LSMO–BFO supercell is shown in figure 4. This heterostructure is half-metallic, with an insulating spin-down band and metallic spin-up band. This is not unexpected as LSMO is a well known half-metal. However, apart from spin-up Mn states at the Fermi-level, we also find a small ($0.01 \mu\text{B}/\text{Fe}$ atom) Fe moment in the spin-up band (i.e. parallel to Mn moment). Layer-specific analysis shows that only the interfacial Fe atoms develop a moment as shown in the inset of figure 4. The plot clearly reveals that both Fe sites have a small DOS in the spin-up band, with a slightly higher DOS (and magnetic moment) at the AF-aligned Fe site than the FM-aligned interface Fe. It is also to be noted that these states appear in the insulating gap of bulk BFO. This moment could be induced from the spin-up Mn states in LSMO (as their evanescent decay tail). The metal-induced gap states [31] causes a net magnetic moment on the first layer of Fe atoms, an observation which is consistent with the experimental result of a BFO magnetic moment close

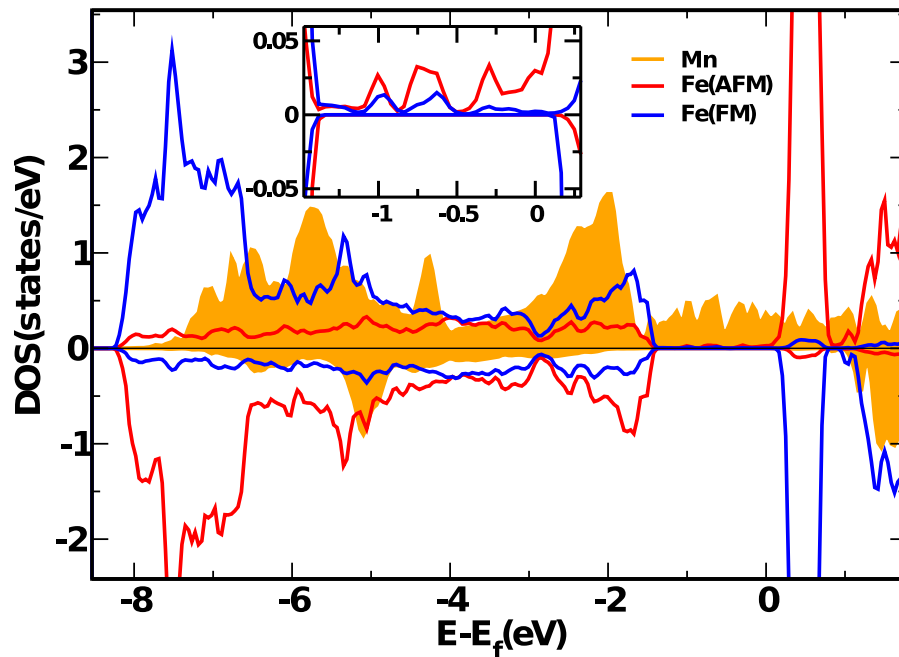


Figure 4. Atom projected DOS for LSMO–BFO. Filled orange curve represents Mn atom of ferromagnetic LSMO, blue and red curves represents Fe atoms of the interfacial BFO layer with Fe spin aligned parallel and antiparallel to Mn spin, respectively. Interface Fe DOS near the band edges is shown in the inset, showing formation of mid-gap states.

to the LSMO–BFO interface. A ferromagnetic coupling is also expected between the interfacial Mn and Fe atoms through oxygen-mediated superexchange interaction, an observation which is consistent with our experimental findings.

5. Conclusion

In conclusion, we have performed a comprehensive, quantitative study of the interfacial charge and spin structure of BFO–LSMO–STO heterostructure. Using the sensitivity of resonant soft x-ray scattering we show that nominally sharp structural interfaces do not necessarily imply a sharp electronic or magnetic interface. We provide quantitative evidence of larger interface roughness and electronic heterogeneity compared to non-resonant characterization methods, a result which compels us to generalize the notion of interface roughness in a broader context beyond sample-specific details. The magnetic depth profile shows that magnetism of LSMO is significantly depleted at the interfaces, particular at the LSMO–STO interface which is consistent with the formation of a magnetically dead layer. Our measurements also reveal that antiferromagnetic BFO develops a very small ferromagnetic moment which peaks very close to the LSMO–BFO interface. Density functional theory assigns it to a proximity-induced charge-transfer process from interfacial Mn to Fe states. On a broader perspective, our findings are useful not only for assessing the potential of these systems for future nano-electronics applications but also provide a new framework with which to enhance our understanding of interface properties using resonant techniques.

Acknowledgments

This work at ALS, MSD at LBNL was supported by the Director, Office of Science, Office of Basic Energy Sciences, of the US Department of Energy under contract no. DE-AC02-05CH11231. Use of the NSLS was supported by the US Department of Energy, Office of Science, Office of Basic Energy Sciences, under contract no. DE-AC02-98CH10886. SK was supported by the US Department of Energy, Office of Basic Energy Sciences, Division of Materials Sciences and Engineering under Award DE-FG02-11ER46831. Work at the University of Alabama was supported by NSF-ECCS grant no. 1102263.

References

- [1] Ohtomo A and Hwang H Y 2004 A high mobility electron gas at the $\text{LaAlO}_3/\text{SrTiO}_3$ heterointerface *Nature* **427** 423
- [2] Caviglia A D, Gariglio A, Reyren N, Jaccard D, Schneider T, Gabay M, Thiel S, Hammer G, Mannhart J and Triscone J-M 2008 Electric field control of the $\text{LaAlO}_3/\text{SrTiO}_3$ interface ground state *Nature* **456** 624
- [3] Reyren N *et al* 2007 Superconducting interfaces between insulating oxides *Science* **317** 1196
- [4] Brinkman A, Huijben M, van Zalk M, Huijben J, Zeitler U, Maan J C, van der Wiel W G, Rijnders G, Blank D H A and Hilgenkamp H 2007 Magnetic effects at the interface between non-magnetic oxides *Nature Mater.* **6** 493
- [5] May S J *et al* 2009 Enhanced ordering temperatures in antiferromagnetic manganite superlattices *Nature Mater.* **8** 892
- [6] Chakhalian J *et al* 2006 Magnetism at the interface between ferromagnetic and superconducting oxides *Nature Phys.* **2** 244
- [7] Chakhalian J, Freeland J W, Habermeier H-U, Cristiani G, Khaliullin G, van Veenendaal M and Keimer B 2006 Orbital reconstruction and covalent bonding at an oxide interface *Science* **318** 1114
- [8] Zheng H *et al* 2004 Multiferroic $\text{BaTiO}_3\text{-CoFe}_2\text{O}_4$ nanostructures *Science* **303** 661
- [9] Manhart J and Schlom D G 2010 Oxide interfaces-an opportunity for electronics *Science* **327** 1607
- [10] Hwang H Y, Iwasa Y, Kawasaki M, Keimer B, Nagaosa N and Tokura Y 2012 Emergent phenomena at oxide interfaces *Nature Mater.* **11** 103
- [11] Lu Y, Li X W, Gong G Q, Xiao G, Gupta A, Lecoer P, Sun J Z, Wang Y Y and Dravid V P 1996 Large magnetotunneling effect at low magnetic fields in micrometer-scale epitaxial $\text{La}_{0.67}\text{Sr}_{0.33}\text{MnO}_3$ tunnel junctions *Phys. Rev. B* **54** R8357
- [12] Bowen M, Bibes M, Barthélémy A, Contour J-P, Anane A, Lemaître Y and Fert A 2003 Nearly total spin polarization in $\text{La}_{2/3}\text{Sr}_{1/3}\text{MnO}_3$ from tunneling experiments *Appl. Phys. Lett.* **82** 233
- [13] Werner R, Yu P A, Alvarez Miño L, Kleiner R, Koelle D and Davidson B A 2011 Improved tunneling magnetoresistance at low temperature in manganite junctions grown by molecular beam epitaxy *Appl. Phys. Lett.* **98** 162505
- [14] Yamada H, Ogawa Y, Ishii Y, Sato H, Kawasaki M, Akoh H and Tokura Y 2004 Engineered interface of magnetic oxides *Science* **305** 646
- [15] Luo W, Pennycook S J and Pantelides S T 2008 Magnetic 'dead' layer at a complex oxide interface *Phys. Rev. Lett.* **101** 247204
- [16] Garcia V, Bibes M, Barthélémy A, Bowen M, Jacquet E, Contour J-P and Fert A 2004 Temperature dependence of the interfacial spin polarization of $\text{La}_{2/3}\text{Sr}_{1/3}\text{MnO}_3$ *Phys. Rev. B* **69** 052403
- [17] Bea H *et al* 2006 Combining half-metals and multiferroics into epitaxial heterostructures for spintronics *Appl. Phys. Lett.* **88** 062502
- [18] Shelke V, Harshan V N, Kotru S and Gupta A 2009 Effect of kinetic growth parameters on leakage current and ferroelectric behavior of BiFeO_3 thin films *J. Appl. Phys.* **106** 104114

- [19] Lukashev P V, Burton J D, Jaswal S S and Tsybmal E Y 2012 Ferroelectric control of the magnetocrystalline anisotropy of the Fe/BaTiO₃(001) interface *J. Phys.: Condens. Matter* **24** 226003
- [20] Mardana A, Ducharme S and Adenwalla S 2011 Ferroelectric control of magnetic anisotropy *Nano Lett.* **11** 3862
- [21] Molegraaf J, Hoffman J, Vaz C, Gariglio S, Marel D, Ahn C and Triscone J 2009 Magnetoelectric effects in complex oxides with competing ground states *Adv. Mater.* **21** 3470
- [22] Wu S M, Cybart S A, Yi D, Parker J M, Ramesh R and Dynes R C 2013 Full electric control of exchange bias *Phys. Rev. Lett.* **110** 067202
- [23] Roy S *et al* 2005 Depth profile of uncompensated spins in an exchange bias system *Phys. Rev. Lett.* **95** 047201
- [24] Kortright J B, Kim S-K, Denbeaux G P, Zeltzer G, Takano K and Fullerton E E 2001 Soft-x-ray small-angle scattering as a sensitive probe of magnetic and charge heterogeneity *Phys. Rev. B* **64** 092401
- [25] Mishra S K, Radu F, Valencia S, Schmitz D, Schierle E, Dürr H A and Eberhardt W 2010 Dual behavior of antiferromagnetic uncompensated spins in NiFe/IrMn exchange biased bilayers *Phys. Rev. B* **81** 212404
- [26] Lee D R, Sinha S K, Haskel D, Choi Y, Lang J C, Stepanov S A and Srajer G 2003 X-ray resonant magnetic scattering from structurally and magnetically rough interfaces in multilayered systems: I. Specular reflectivity *Phys. Rev. B* **68** 224409
- [27] Parratt L G 1954 Surface studies of solids by total reflection of x-rays *Phys. Rev.* **95** 359
- [28] Nevot L and Croce P 1980 Characterization of surfaces by grazing incidence x-ray reflection-application to the study of polishing of some silicate glasses *Rev. Phys. Appl.* **15** 76
- [29] Valvidares S M, Huijben M, Yu P, Ramesh R and Kortright J B 2010 Native SrTiO₃(001) surface layer from resonant Ti L_{2,3} reflectance spectroscopy *Phys. Rev. B* **82** 235410
- [30] Borisevich A Y *et al* 2010 Suppression of octahedral tilts and associated changes in electronic properties at epitaxial oxide heterostructure interfaces *Phys. Rev. Lett.* **105** 087204
- [31] Heine V 1965 Theory of surface states *Phys. Rev.* **138** A1689